Received: 26 June 2021 | Revised: 24 July 2022 | Accepted: 18 September 2022

DOI: 10.1002/ls.1629

RESEARCH ARTICLE

WILEY

Flow and slip process of Santotrac 50-based lubricant under high shear by molecular dynamic simulation

Xin Zhao[1,2] | Chao Wei[1] | Zhenxin Yin[1] | Wenjie Ma[3]

[1]National Key Laboratory of Vehicular Transmission, Beijing Institute of Technology, Beijing, People's Republic of China

[2]State Key Laboratory of Nonlinear Mechanics, Institute of Mechanics, Chinese Academy of Sciences, Beijing, People's Republic of China

[3]Département de Physique, de Génie Physique et d'Optique, Université Laval, Quebec City, Quebec, Canada

Correspondence
Chao Wei, National Key Laboratory of Vehicular Transmission, Beijing Institute of Technology, Beijing, People's Republic of China.
Email: weichaobit@163.com

Funding information
National Natural Science Foundation of China, Grant/Award Number: 51875039

Abstract

We investigate flow and slip behaviour of Santotrac 50 molecules under high shear in Couette cell by means of Molecular Dynamic simulation to understand reduced friction force. Molecular chain stretches and oriented to shear direction, and move. Slip starts on metal surface at 2×10^8 s^{-1}, and increases with shear rate. Slip length keeps scale at nanometre. Molecular conformation and occurrence of slip both indicate a reduced shear stress. Furthermore, when changing wettability, slip length increases in power law and thus decreases shear stress greatly. Occurrence of low-density region near surface can explain slip. And thus, we extended apparent slip model, which divided lubricant into liquid layers with different viscosities, to elucidate the relationship between molecule distribution inner layer and slip on surface influenced by shear velocity and wettability. Above all, our research sheds light on flow and slip behaviour of complex fluid and can be applied in improving lubrication property.

KEYWORDS

carbon-chain lubricant, high shear rate, molecular dynamics simulation, slip

1 | INTRODUCTION

Organic liquids are commonly used in engineering lubrication, for instance, lubricants can form efficient lubricant films between mechanical shear pairs to maintain operation at a very low friction even at high rotation speed and high pressure, such as gear,[1–3] seal ring,[4–7] wet clutch,[8,9] and so forth.

Compared with simple, inorganic liquid, present complex force response to external stimuli since the carbon chain reacts differently with surrounding, such as, deformation, tilt, reorientation, and so forth, and thus results in various phenomena. In early 1990s, Boersma et al. reported a clear slipping plane just above the surface in a Couette system filled with shear-thickened solution at a relatively high shear rate.[10] Linear extrapolation in velocity close to interface is hence invalid due to the formation of inconsistent molecular density distribution near wall.[11,12] Once slip happens, nominal shear rate is larger than real shear rate acting on lubricant, indicating lubrication promotion and friction reduction. Besides, in many cases, lubricant film is typically at the mesoscale of around 0.1 μm ∼ several μm at which slip probably gives effect.[13,14] Therefore, in such situation, slip phenomenon should be considerately considered in thin film lubrication. Since slip occurs within boundary layer, and the shear-induced change in molecular structure happens both in the bulk and boundary, there exists other reasons to cause the occurrence of slip. Thus to observe molecular motion of chain behaviour in vicinity of interface can be helpful to understand slip under high shear and pressure, which may be useful to explain the reduced shear force in lubrication.

Recent experiments have realised the direct observation of velocity profile in the range of within 1 μm above interface in the water,[15–17] but it is still difficult to detect flow feature of complex fluid in vicinity of interface. However, Molecular Dynamic simulation (MDs)

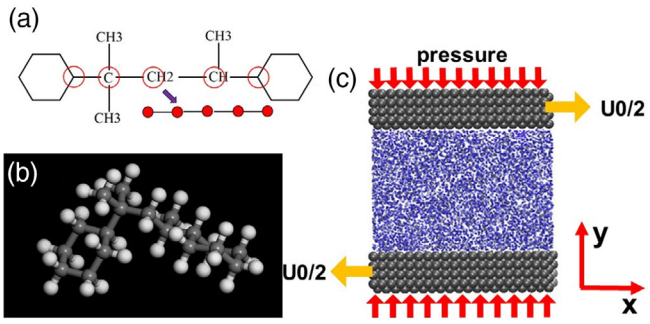

FIGURE 1 (a) Formula and (b) 3D structure of C18H34 molecule; (c) Couette flow in MDs

advances in analysing the chain configuration and the motion of single molecule during shear, and thus help understand the rich and unusual flow property at the time scale and molecular level.[18–22] For example, the topology constraint of entangled chains limits their movement due to the fact of their tight connection to another monomer.[21] Specially, the introduction of boundary influences the molecular properties differing from bulk. Besides, using MDs, the dissolution of liquid at interface can be imitated, and a flow pattern changing from plug-like to Poiseuille-like can be observed with the increase of dissolubility.[22]

In this paper, we investigate molecular behaviour of organic lubricant, Santotrac 50, under high shear and different pressures via MDs. Carbon chain stretches and orients towards external shear, and thus the viscosity changes. A larger pressure makes molecular configuration more ordered. Concurrence of slip and molecular rearrangement by external shear both results in reduced shear force. By tuning the shear velocity and wettability, the slip length increases. The apparent slip model, which simplifies the lubricant into liquid layers with different viscosities parallel to plane, have been applied to give qualitative explanation to the influence of shear velocity and wettability on slip. Our research gives molecular understanding on the flow and slip processes of complex fluid under high shear rate, and is potential in lubrication application.

2 | SHEAR PROCESS BY MOLECULAR DYNAMIC SIMULATION

2.1 | Modelling

The Santotrac 50 (C18H34, CAS:38970-72-8)[23] composes of about 70% ~ 99% of one general tractive oil, and thus we think it contributes to the main flow characteristics of such oil. For simplification, we choose Santotrac 50 as the single phase to simulate the flow behaviour in our simulation. The formula and 3D Santotrac 50 molecule are shown in Figure 1a,b. The Santotrac 50 molecule is simulated in all-atom model, which means all 18 molecules have been considered. In order to clearly describe the change of chain configuration during dynamic process, five carbon balls connected with stick is given to describe carbon in main chain. Two benzene rings are simplified to be two carbon balls corresponding to the carbon atom connected at the main chain. Such simplification is called as 'five-carbon ball-and-stick model'. And it is used in capturing the characteristics of molecular motion and its conformation, which can be shown in Figure 2.

The system is composed of two planes and a lubricant layer which is inserted between planes (as shown in Figure 1c). Each plane, made of 3200 *F*e arranged in BCC lattice, is at the size of 11.4656 Å × 57.328 Å × 57.328 Å. The lubricant is composed of 400 Santotrac 50 molecules. The Lennard-Jones 9–6 potential function is chosen to describe interaction between molecules.[24]

$$U_{ij}\left(\vec{r}_i,\vec{r}_j\right)=c\varepsilon_{ij}\left[2\left(\frac{\sigma_{ij}}{r_{ij}}\right)^9-3\left(\frac{\sigma_{ij}}{r_{ij}}\right)^6\right], \tag{1}$$

in which c, the relative energy coefficient, is used to adjust the wettability of *F*e plane. ε_{ij}, σ_{ij} and r_{ij} indicate the depth of potential well, the effective molecular diameter, and the distance between two atoms i and j, respectively. In our simulation, intermolecular parameters ε_{ij} and σ_{ij} can be expressed by single molecule parameters, that is,

$$\begin{cases}\varepsilon_{ij}=\dfrac{\left(2*\sqrt{\varepsilon_i*\varepsilon_j}\right)*\sigma_i^3*\sigma_j^3}{\left(\sigma_i^6+\sigma_j^6\right)}\\ \sigma_{ij}=\left[\dfrac{\left(\sigma_i^6+\sigma_j^6\right)}{2}\right]^{\frac{1}{6}}\end{cases}. \tag{2}$$

The shear force is applied by two-plane moving opposite at velocity of $U_0/2$ and thus shearing the lubricant. A periodic boundary is set on two ends. Verlet method[25] is commonly applied to generate approximate solutions to Newton's second law for position-dependent forces. The temperature was controlled at 300 K with a Nosé–Hoover thermostat with relaxation time 0.5 ps.[26]

2.2 | Molecular motion under shear

The carbon chain of lubricant can be elongated by external shear and thus reduces the entanglement between

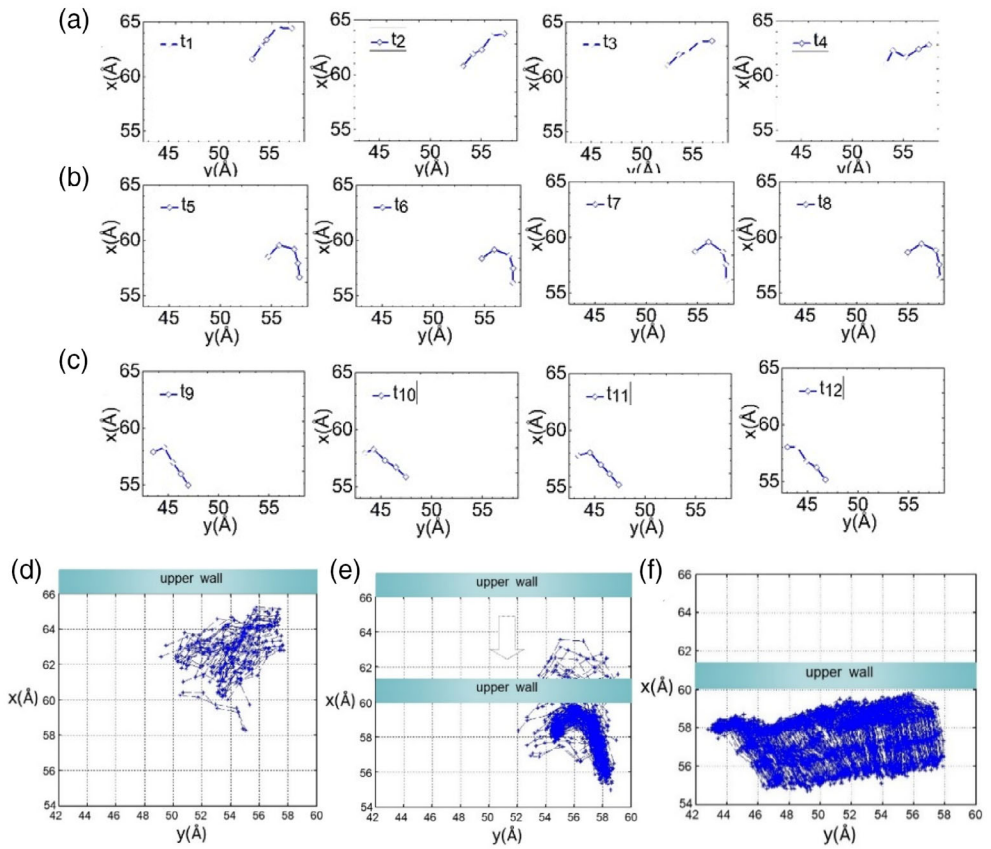

FIGURE 2 Frame image of single molecule: (a) relaxation with zero pressure; (b) under a higher pressure (nominal pressure 1.55 GPa set in simulation); (c) under a higher pressure (nominal pressure 1.55 GPa set in simulation) with shear velocity of 5 m/s; molecular trajectory in different stages of (d) relaxation with zero pressure; (e) under a higher pressure (nominal pressure 1.55 GPa set in simulation); (f) under a higher pressure (nominal pressure 1.55 GPa set in simulation) with shear velocity of 5 m/s

bodies. The configurations varying with shear will be strongly connected to the flow. In order to look into the molecular posture with external stimulus in one simulation, we extract three stages: (i) relaxation with zero pressure (nominal pressure 0 GPa set in simulation); (ii) under a higher pressure (nominal pressure 1.55 GPa set in simulation); (iii) under a higher pressure (nominal pressure 1.55 GPa set in simulation) and shear velocity at 5 m/s. Each stage is at thermal equilibrium.

In Figure 2a–c, we extract frame image per 5 ps for one molecule to record its posture and position in three stages. We can see that, in the relaxation stage, Santotrac 50 molecules are distanced from each other and thus molecules are not confined greatly. Thus, in Figure 2a, Santotrac 50 molecule can change posture obviously and moves relatively freely. The molecular posture in this stage is unfold. In Figure 2b, under a higher pressure, the space between molecules decreases greatly, and thus each molecule is difficult to move. Additionally, from 3D molecule in Figure 1b, we can see Santotrac 50 molecule prefers to bend to optimise its energy and thus it maintains the bending shape due to confinement, but still vibrates around a limited space due to thermal fluctuation (as indicated in the overlapped frames Figure 2e). If shear is applied, carbon chain is stretched by shear of adjacent molecule and thus tend to move parallel to the plane. The motion is directional, and its component vertical to plane is very weak. A linear chain structure usually indicates less entanglement during movement and thus a decreased viscosity.

We further overlap large amounts of frames to draw molecular trajectory in three stages. It is clear that in relaxation status (as indicated in Figure 2d), Santotrac 50 molecule moves randomly and it behaves like fluid. Specially, we extract the molecular configuration change when pressure is gradually applied. It can be seen in Figure 2e, the space for a molecule to move is shrinking rapidly. The configuration of molecule changes from chaos to quite uniform. Finally, the molecule is confined to only vibrate slightly around itself. In the shear case (in Figure 2f), the molecule moves almost linear along shear direction. Since there exists velocity difference between two molecules at two different heights, their distance will become further with time which means molecules at one layer sliding over another. Such slide-like motion indicates solid-like behaviour. Such behaviour is typical at high shear rate. Considering the molecules can move, Santotrac 50 bulk still keeps in liquid state. Actually, many rheological experiments observed non-Newtonian behaviour for complex fluids under high shear.

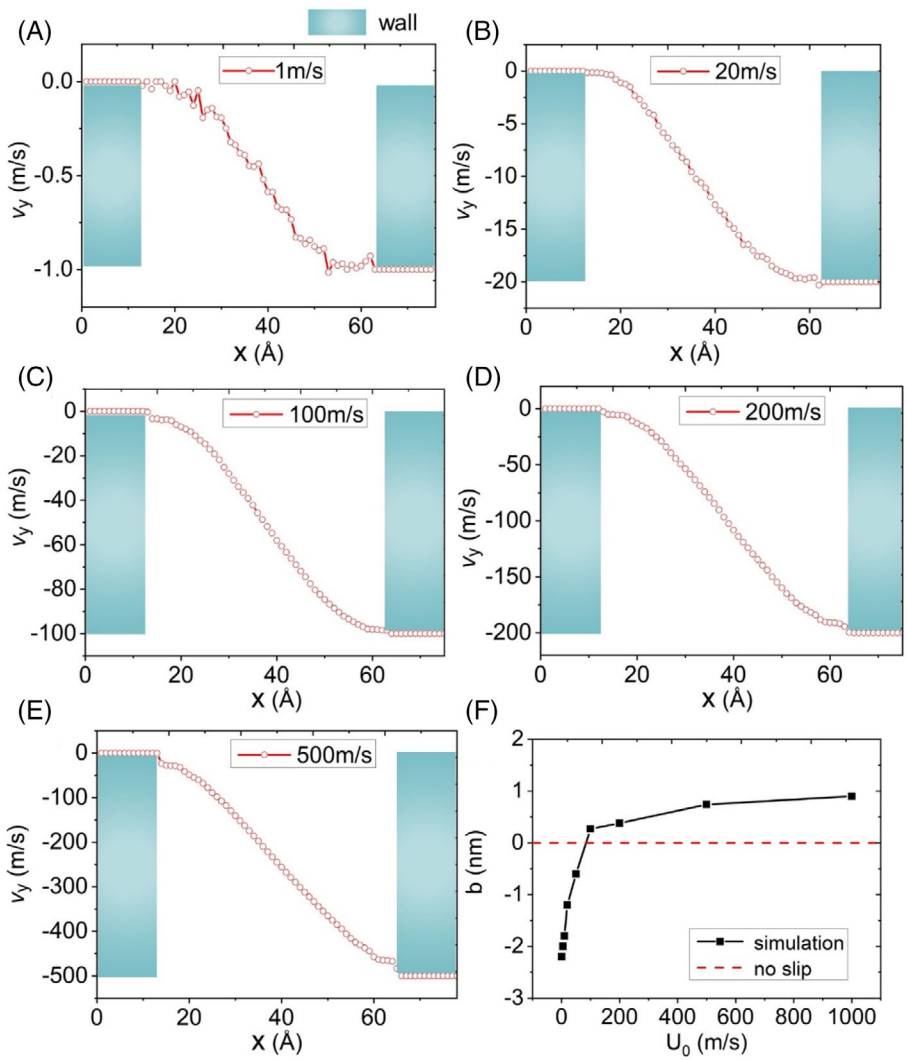

FIGURE 3 Velocity distribution of Santotrac 50 molecules (a) at 1 m/s; (b) at 20 m/s; (c) at 100 m/s; (d) at 200 m/s; (e) at 500 m/s; (f) slip length vs shear velocity

2.3 | Slip under high shear

In the following, we simulate shear process at a higher pressure (1.55 GPa in simulation) and 300 K with shear rate ranging from 2×10^8 s^{-1} to 10^{11} s^{-1}. The velocity profile is obtained by statistically averaging velocity at certain positions. A velocity jump appears at about $2 \sim 3$ Å away from plane, which is about one length scale of $C_{18}H_{34}$. We extract the slope of two jump velocity at two ends to extrapolate to the solid, and the distance between the intersection and the surface is the slip length. It can be seen that slip starts at 100 m/s (2×10^{10} s^{-1}), and the velocity jump value increases with shear rate, as indicated in Figure 3c–e. Overall, the slip length in our simulation is less than 2 nm in Figure 3f. Actually, based on the reported experiment data, the measured slip length on hydrophilic surface is about ~nm,[27] so our simulation data is reasonable compared to experiment. Since the slip length is close in magnitude to the distance between two planes (~5 nm), the influence of slip on flow and shear stress should be considered.

In Figure 4a–d, we look deeply into the density distribution between two planes that, a strong density fluctuation also appearing in vicinity of plane ($2 \sim 3$ Å) indicates a corresponding relationship between slip and local density. It is obvious that in Figure 4a–d there exists a depletion layer with a very low molecule density right above the surface and then followed by a higher density part. Moreover, the simulation seems that the velocity does not change the density distribution close to interface greatly before and after slip, but velocity does influence the density fluctuation in the bulk phase, and a higher shear rate decreases the density fluctuation in the liquid. Thus, it is possible that the velocity influences the nominal boundary between depletion layer and bulk.

Since density is proportional to viscosity, we thus introduce apparent slip model which is composed of two

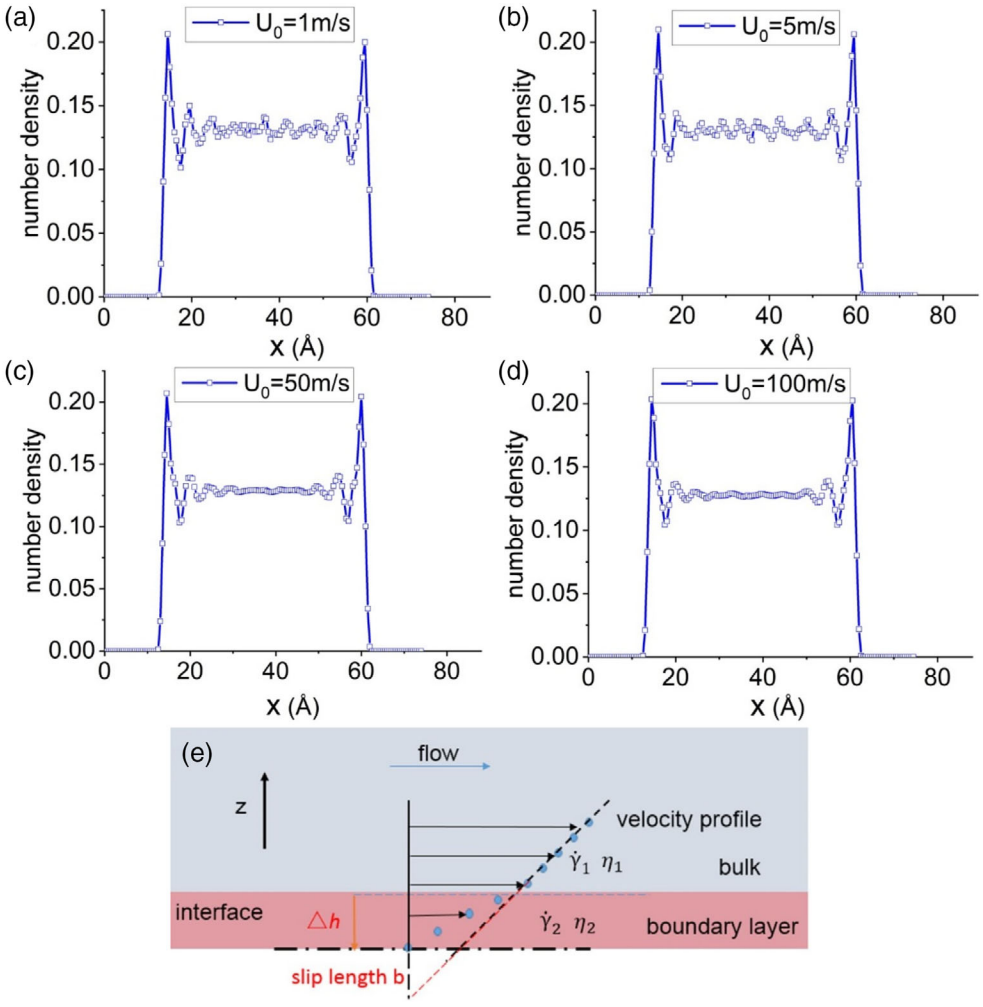

FIGURE 4 (a) Density distribution for 400 molecules under pressure (1.55 GPa in simulation) and velocity of (a) 1 m/s; (b) 5 m/s; (c) 50 m/s; (d) 100 m/s; (e) apparent slip model introduction

layers of different viscosities above the surface to explain the occurrence of slip here. Assuming that plane is covered by a boundary layer of low viscosity, η_2, and above the bulk of high viscosity, η_1 (the peak density is allocated to the bulk layer), the shear rates for two media are $\dot{\gamma}_1$ and $\dot{\gamma}_2$, respectively (as shown in Figure 4e). If the thickness of boundary layer is Δh , and the velocity on the top of boundary layer is U, thus a relationship with slip length b can be given according to velocity continuity and Navier slip model,[28]

$$U = \dot{\gamma}_1 \times (b + \Delta h) = \dot{\gamma}_2 \times \Delta h. \tag{3}$$

Considering a force equilibrium relationship,

$$\dot{\gamma}_1 \times \eta_1 = \dot{\gamma}_2 \times \eta_2. \tag{4}$$

The slip length can be expressed by viscosity ratio and thickness Δh.

$$\frac{(b + \Delta h)}{\Delta h} = \frac{\dot{\gamma}_2}{\dot{\gamma}_1} = \frac{\eta_1}{\eta_2} = \text{constant}. \tag{5}$$

Due to a depletion layer appearing right on the plane, the viscosity is very tiny for all shear situations. It is reasonable to assume it to be constant but small enough. The bulk viscosity will vary with shear due to the shear changing molecular configuration. But there exists a final molecular state under high shear when all molecules finish the orientation. With the increase of shear, more molecules change its configuration to the final state under high shear and less entanglements in system, thus here for the simplification, we assume bulk viscosity to be a constant. We notice that the velocity fluctuation for small shear velocity is large, which indicates an ambiguous edge between bulk and boundary layer. With the increase of shear velocity, the edge becomes clear due to external shear, thus the Δh becomes small at high shear. Moreover, concurrent of slip is reported to be a result of overcome defeat of large domain by large external force,[29] and thus, large external shear indicates a clear slip plane and then an increase in slip length. A slip length model proposed by Thompson and Troian[30] using MDs, $b = b_0/\left(1 - \dot{\gamma}\dot{\gamma}_c^{-1}\right)^{0.5}$, predicts power-law rise exceeding a

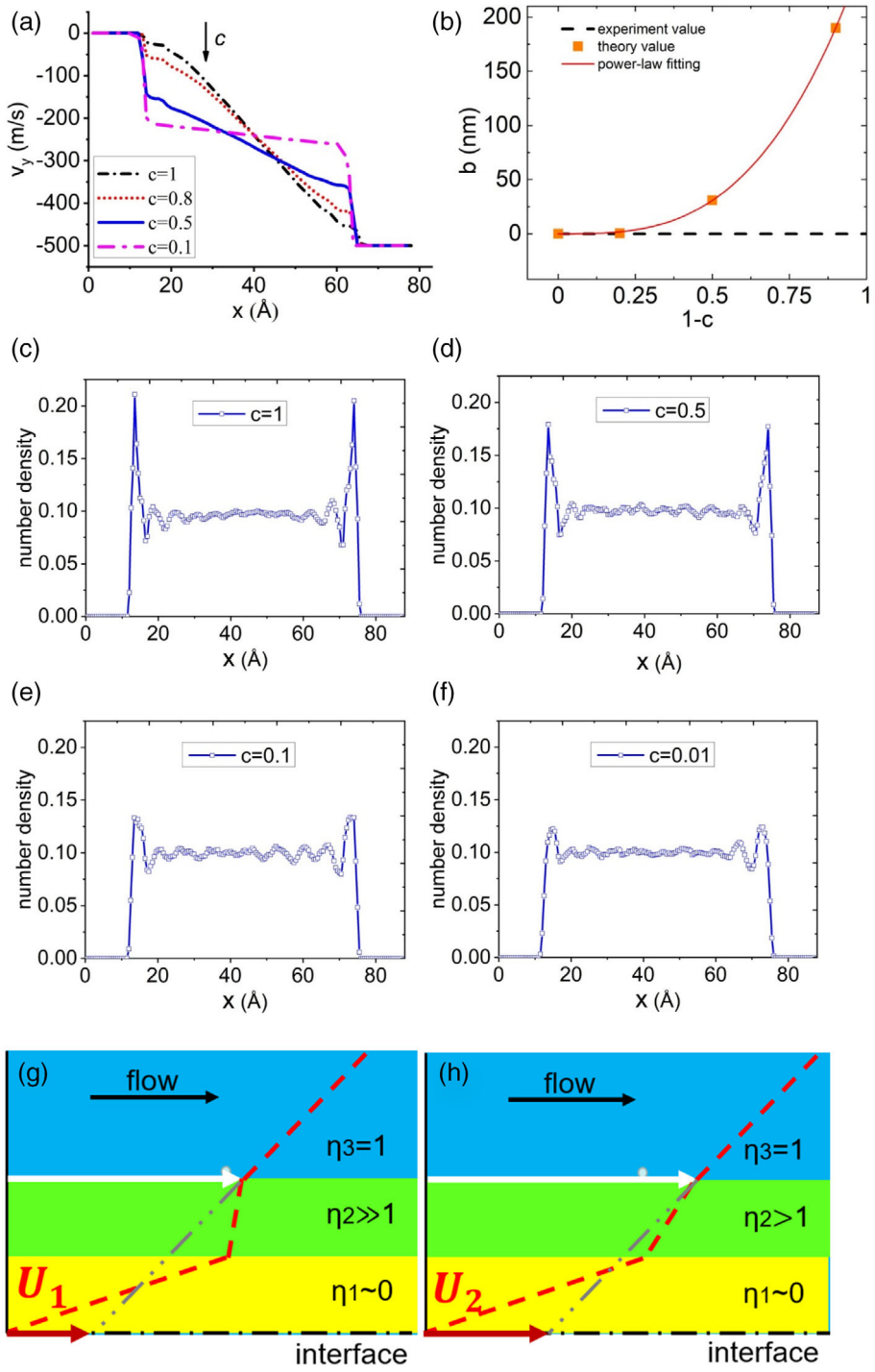

FIGURE 5 (a) Velocity distribution vs wettability; (b) slip length versus c; density distribution for different c. (c) $c = 1$; (d) $c = 0.5$; (e) $c = 0.1$; (f) $c = 0.01$; three-layer apparent slip model of (g) weak wettability and (h) strong wettability

critical shear rate $\sim 10^{11}\,s^{-1}$. A later work by Lichter et al.[29] believes slip length will face an upper limit with the increase of external force strength due to its relation to defeat number. We did not see clear increase in slip length with shear rate in our simulation, maybe because the interaction between complex liquid molecules is still stronger under high shear than that in liquid of simple molecules.

3 | APPLICATION DISCUSSION: FRICTION REDUCTION WITH WETTABILITY-RELATED SLIP

In our previous discussion, slip between friction pair can efficiently decrease shear stress at high shear rate and thus increases lubrication. Therefore, if some available measures can be taken to increase slip further, the

lubrication can be improved. From the perspective of surface science, according to Young-Laplace equation, non-wetting indicates low surface energy and weak adhesion. An intuition is that a weak adhesion reflects the easy-flow property for liquid. Additionally, surface can be easily treated in various physical and chemical ways to change surface energy, and as well different materials can present different surface energies. By utilising surfaces with low energy, the friction between tractive pair is predicted to decrease. Thus, in this part, we simulate influence of wetting on slip by the MDs and hopefully make it as a potential way for better performance in lubrication.

The wetting can be adjusted by relative energy coefficient, c, and the smaller the weaker interaction between molecules. We simulate c at 0.01, 0.1, 0.5, 0.8 and 1. Clearly in Figure 5b, slip length increases with the decrease of c. When the $c < 0.5$, the slip length increases approximately to power law.

We extract the density distribution for different surface wetting conditions. A tendency is that to decrease relative energy coefficient decreases the density peak in vicinity of surface, which indicates actually a weak adhesion (Figure 5c–f). Similarly, we also apply the apparent slip model to explain such principles. In order to describe the variation of peak density, a layer with higher viscosity is specifically defined. Thus, in this situation, we assume three layers with different viscosities, η_1, η_2 and η_3, from down to up. The first layer is depletion layer with a viscosity $\eta_1 \sim 0$ and the third layer is the bulk with a viscosity $\eta_3 \sim 1$. Then according to the variation of density peak, we define two situations with $\eta_2 > 1$ and $\eta_2 \gg 1$ for small and high peaks, separately (as indicated in Figure 5g,h). Same shear stress is applied in two situations, and then a larger slip velocity and flux appear in the case with $\eta_2 > 1$, which corresponds to small peak. Therefore, a decrease in wetting decreases the adhesion, and thus increases the slip.

Recent experimental evidence shows clearly the friction in the EHL regime can be reduced a lot by tailoring the wetting and surface energy. In Polajnar and Kalin' work, the contact pairs made of different materials were tested to analyse the relationship between surface energy and friction. The experimental results showed that the coefficient of friction can be decreased a lot in a surface with low energy.[31,32] They concluded that poor wetting with low surface energy, for example, low spreading parameter, can lead to easier slip. Their experiments well coincide with our simulation.

4 | CONCLUSION

To summary, in this paper, we simulate the Couette flow of Santotrac 50 under high shear rate over $2 \times 10^8\ s^{-1}$ and different pressures via Molecular Dynamics simulation, and investigate the molecular structure changing with pressure and shear rate. The results indicate that the molecular structure turns to consistence under pressure and chain will stretch and move in the direction of shear. Meantime, clear velocity jump occurs when shear rate reaches $2 \times 10^{10}\ s^{-1}$, indicating tiny slip length, ~nm, on metal surface. In such situation, friction can be reduced by concurrence of slip and molecular rearrangement by external shear. Besides, the influence of wettability on slip has been discussed and a power-law increase in slip length has been observed. The occurrence of slip can be explained by changes in surface induced deletion layer. We applied the apparent slip model, which considers lubricant as liquid layers with different viscosities, to explain the influence of surface and wettability and shear velocity on particle number density on slip qualitatively. Thus, available measures can be taken to increase slip, for example, changing property of surface to reduce friction. This research helps elucidate non-Newtonian rheological behaviour for complex liquid at high shear rate at a molecular scale and is useful for understand EHD lubrication.

ACKNOWLEDGEMENTS

The research has been funded by the National Natural Science Foundation of China (Grant 51875039). The Chinese Scholarship Council is acknowledged for funding.

DATA AVAILABILITY STATEMENT

Data available in article supplementary material.

ORCID

Xin Zhao https://orcid.org/0000-0003-4876-079X

REFERENCES

1. Dong HL, Hu JB, Li XY. Temperature analysis of involute gear based on mixed elastohydrodynamic lubrication theory considering tribo-dynamic behaviors. *J Tribol*. 2014;136(2):021504.
2. Yilmaz M, Kratzer D, Lohner T, Michaelis K, Stahl K. A study on highly-loaded contacts under dry lubrication for gear applications. *Tribol Int*. 2018;128:410-420.
3. Zhang JG, Liu SJ, Fang T. On the prediction of friction coefficient and wear in spiral bevel gears with mixed TEHL. *Tribol Int*. 2017;115:535-545.
4. Zhao X, Yuan SH, Chao W. Influence of fluid slip on operation characteristics for high-speed spiral groove seal ring. *Tribol Lett*. 2018;66(1):49.
5. Xue B, Wei C, Hu JB. Study of separation characteristics of micro-groove rotary seal considering different cavitation boundary conditions. *Tribol Lett*. 2017;65(4):119.
6. Xue B, Wei C, Hu JB. Research on effects of groove shape optimization on cavitation and lubricating characteristics for micro-grooves rotary seal. *Tribol Trans*. 2018;61(3):569-584.

7. Zhao YM, Yuan SH, Hu JB, et al. Nonlinear dynamic analysis of rotary seal ring considering creep rotation. *Tribol Int*. 2015; 82, Part A:101-109.
8. Zhang L, Wei C, Hu JB, Hu Q. Nonlinear dynamic characteristics of rub-impact process at high circumferential velocities in no-load multiplate wet clutch. *Tribol Trans*. 2019;10:1-19.
9. Zhang L, Wei C, Hu JB, Hu Q. Influences of lubrication flow rates on critical speed of rub-impact at high circumferential velocities in no-load multi-plate wet clutch. *Tribol Int*. 2019;140:105847.
10. Boersma WH, Baets PJM, Lavèn J, et al. Time-dependent behavior and wall slip in concentrated shear thickening dispersions. *J Rheol*. 1991;35(6):1093-1120.
11. Ya MA, Patlazhan SA. Wall slip for complex liquids – phenomenon and its causes. *Adv Colloid Interface Sci*. 2018;257:42-57.
12. Zhao X, Wei C, Yuan SH. Determination of slip length in Couette flow based on an analytical simulation incorporating surface interaction. *Chin Phys Lett*. 2017;34(3):034701.
13. Bhattacharyya K, Mukhopadhyay S, Layek GC. Slip effects on an unsteady boundary layer stagnation-point flow and heat transfer towards a stretching sheet. *Chin Phys Lett*. 2011;29(9):094702.
14. Zhao X, Chao W, Shihua Y. Slip in Couette flow with pressure gradient: theoretical and experimental investigation of hydrodynamic characteristics considering slip effect. *J Hydrodyn*. 2020;32(1):107-115.
15. Zhao X, Best A, Liu W, Koynov K, Butt HJ, Schönecker C. Irregular, nanostructured superhydrophobic surfaces: local wetting and slippage monitored by fluorescence correlation spectroscopy. *Phys Rev Fluids*. 2021;6(5):054004.
16. Schffel D, Koynov K, Vollmer D, et al. Local flow field and slip length of superhydrophobic surfaces. *Phys Rev Lett*. 2016; 116(13):134501.
17. Vinogradova OI, Koynov K, Best A, Feuillebois F. Direct measurements of hydrophobic slippage using double-focus fluorescence cross-correlation. *Phys Rev Lett*. 2009;102(11):118302.
18. Huang DM, Sendner C, Horinek D, Netz RR, Bocquet L. Water slippage versus contact angle: a quasiuniversal relationship. *Phys Rev Lett*. 2008;101(22):226101.
19. Kioupis LI, Maginn EJ. Impact of molecular architecture on the high-pressure rheology of hydrocarbon fluids. *J Phys Chem B*. 2000;104(32):7774-7783.
20. Priezjev NV. Relationship between induced fluid structure and boundary slip in nanoscale polymer films. *Phys Rev E*. 2010;82: 051603.
21. Kremer K, Grest GS. Dynamics of entangled linear polymer melts: a molecular-dynamics simulation. *J Chem Phys*. 1990; 92(8):5057-5086.
22. Miao Q, Yuan Q, Zhao YP. Dissolutive flow in nanochannels: transition between plug-like and Poiseuille-like. *Microfluid Nanofluidics*. 2018;22(12):141.
23. Material Satety Data Sheet [EB/OL]. [2013-08-21]. http://www.santolubes.com/resources/tds-msds/MSDS-SANTOTRAC-50.pdf
24. Lennard-Jones JE. Cohesion. *Proc Phys Soc*. 1931;43:461-482.
25. Verlet L. Computer experiments on classical fluids. I. Thermodynamical properties of Lennard-Jones molecules. *Phys Rev*. 1967;159:98-103.
26. Nosé S. A unified formulation of the constant temperature molecular dynamics methods. *J Chem Phys*. 1984;81:511; Hoover WG. *Phys Rev A*. 1985;31:1695.
27. Bonaccurso E, Kappl M, Hans-Jürgen B. Hydrodynamic force measurements: boundary slip of water on hydrophilic surfaces and electrokinetic effects. *Phys Rev Lett*. 2002; 88(7):076103.
28. Navier C. *Memoires de l'Academie Royale des Sciences de l'Institut de France*. Vol 6. Academie Royale Des Sciences; 1823:389.
29. Lichter S, Roxin A, Mandre S. Mechanisms for liquid slip at solid surfaces. *Phys Rev Lett*. 2004;93:086001.
30. Thompson PA, Troian SM. A general boundary condition for liquid flow at solid surfaces. *Nature*. 1997;389:360-362.
31. Kalin M, Polajnar M. The wetting of steel, DLC coatings, ceramics and polymers with oils and water: the importance and correlations of surface energy, surface tension, contact angle and spreading. *Appl Surf Sci*. 2014;293:97-108.
32. Kalin M, Polajnar M. The effect of wetting and surface energy on the friction and slip in oil-lubricated contacts. *Tribol Lett*. 2013;52(2):185-194.

How to cite this article: Zhao X, Wei C, Yin Z, Ma W. Flow and slip process of Santotrac 50-based lubricant under high shear by molecular dynamic simulation. *Lubrication Science*. 2023;35(3):163-170. doi:10.1002/ls.1629